Research Article

Novel cancer associated fibroblasts from diverse locales enhance the tumorigenicity of tongue tumor epithelia

Nehanjali Dwivedi[1,2#], Hafsa Bahaar[1#], DN Shashank[1#], Christine Elizabeth Cherry[1], Charitha Gangadharan[3], Amritha Suresh[4], Moni A Kuriakose[5], Vijay Pillai[5], Smitha PK[6], and Manjula Das[1*]

Abstract

Due to high rates of tobacco chewers, smokers, and alcohol consumers in India, Head and Neck Squamous Cell Carcinoma (HNSCC) is one of the primary causes of mortality. Being profoundly varied in nature, treating patients diagnosed with HNSCC can be difficult. An invitro cell line model is needed to better comprehend the heterogeneity especially via the interaction with components of the microenvironment like Cancer Associated Fibroblasts (CAFs). The effectiveness of creating cell lines from head and neck cancers is, however, poor. Furthermore, except for the two reported earlier by the authors, no other immortalized CAF cell lines are available to study the cross-talk of the tumor with its microenvironment. In this study, the authors report three novel CAF lines, spontaneously immortalized, from Human Papilloma Virus (HPV) negative male patients with habits of tobacco and diagnosed with squamous cell carcinoma of the upper alveolus, larynx and buccal mucosa. Negative staining with EpCAM, CD31 and CD45, while positive staining with FSP-1 determined their fibroblast specific lineage. Interestingly, in indirect co-culture experiments all three CAFs, though isolated from tumors of different regions of the oral cavity, could increase the tumorigenicity of the epithelial cells from tongue-tumor indicating at a common "CAF-factor". The developed CAF cell lines are the first of their kind from the mentioned sites, and can act as invaluable tools for learning the site-independent common language between tumor-stroma and tumor in HNSCC.

Affiliation:

[1]Molecular Immunology, MSMF, Narayana Health City, Bangalore 560099, India.

[2]MAHE, Manipal, 576104, India.

[3]Department of Clinical Research, Mazumdar Shaw Medical Centre, Narayana Health City, Bangalore 560099, India.

[4]Integrated Head and Neck Oncology Research, MSMF, Narayana Health City, Bangalore 560099, India.

[5]Department of Head and Neck Surgery, Mazumdar Shaw Medical Centre, Narayana Health City, Bangalore 560099, India.

[6]Product Research Group, MSMF, Narayana Health City, Bangalore 560099, India.

[#]Equal contribution

*Corresponding author:
Manjula Das, Molecular Immunology, MSMF, Narayana Health City, Bangalore 560099, India.

E-mail: manjula.das@ms-mf.org

Keywords: Head and Neck Squamous Cell Carcinoma; Cancer-associated fibroblasts; Novel cell line; Upper alveolus; Larynx; Buccal mucosa and Tongue epithelia

Introduction

Head and Neck Squamous Cell Carcinoma (HNSCC), the seventh most common cancer worldwide, accounts for more than 325,000 mortalities and 660,000 new incidences across the world [1,2]. However, in India it is the most prevalent form of male cancer, may be owing to the population's extensive oral habits of areca nut, lime and tobacco chewing in addition to smoking and drinking [3,4]. Infection with the Human Papilloma Virus (HPV) has been linked to an increased risk of HNSCC [5-7]. In India, the 5-year survival rates for patients with HNSCC at the early and advanced stages are 82 and 27%, respectively [8]. The five-year survival rate of patients with HNSCC is still low due to distant metastasis and recurrence, and the patient's quality of life has remained a severe issue despite advances in early detection and therapy [9,10]. Therefore, a deeper comprehension of the intricate etiology of HNSCC is required to create a more potent treatment. An essential part

of the growth of tumors is the extracellular matrix (ECM), the macromolecule-rich tumor microenvironment (TME). It is now understood that cell interactions within the tumor microenvironment play a key role in tumor development and progression [11]. Fibroblasts are the second most common type of cells in the microenvironment and are a dynamic population of cells with a wide range of phenotypic and functional characteristics. Nearly all solid tumor tissues include CAFs, which significantly influence the malignant development of cancer, including metastasis and the epithelial-to-mesenchymal transition (EMT) [12]. CAFs, therefore can be viewed as "the other side of the coin" in tumorigenesis [13]. Cell lines remain a valuable resource for performing translational research in laboratory settings despite the challenges of long-term preservation[14]. Establishment of primary cultures enables investigation into the parent tumor's microenvironment-driven traits. Additionally, it is imperative to create and characterize novel CAF lines from patient malignancies due to the dearth of commercially available CAFs. A key tool for improving our understanding of tumor heterogeneity and stroma-tumor cross-talk is *in vitro* cell-based models of cancer [15-17]. Tatake *et al.,* discuss the development of epithelial cell lines from the lower alveolus, buccal mucosa, gingivobuccal mucosa, oral cavity, tongue, sinonasal, pyriform, and retromolar trigone in the treatment of head and neck cancer [18]. Eighty five cell lines from distinct head and neck locations were further assembled and described by Zhao et al. in 2011 [19]. Hayes et al. previously produced 16 cell lines from patients with HNSCC to better understand the effects of various mutations on tumor behavior [20]. Various studies have reported isolation of CAF primary cultures from different sites of oral cavity, gingivo-buccal mucosa [21], tongue, retromolar area, palate [22] and other regions such as lip, jaw, soft palate etc [23-25]. The authors of this study, for the first time have reported the establishment of immortalized CAF-cell lines from tongue carcinoma [26]. In the current study, CAFs have been immortalized from tobacco-user, HPV negative male patients diagnosed with moderately differentiated squamous cell carcinoma of the larynx, upper alveolus and buccal mucosa. Their overt ability to increase the tumorigenicity of the epithelial cell

lines from tongue-tumor [26] indicate the existence of a common language of CAF-factor between the stroma and tumor in HNSCC. These set of CAF cell lines along with the previously described autologous pairs expand a novel *in-vitro* platform to study the science of tumor-stroma cross talk.

Materials and Methods

Tumor sample collection and cell line establishment

Tumor samples were collected from three different patients diagnosed with moderately differentiated squamous cell carcinoma, after receiving the patient's informed consent form. The current study was approved by the Narayana Health City ethics committee with an approval number – NHH/MECCL2015405 (A) from Bengaluru, India. Tumor samples were collected in sterile RPMI-1640 (cat. no. AT222A; HiMedia Laboratories; LLC) supplemented with 3X Penicillin-Streptomycin solution (#15140122; Gibco; Thermo Fisher Scientific, Inc.) from two males with habits of drinking, chewing and smoking, while for one of the patients, the habits were not reported. Patients MhCL03-F, MhCA04-F, and MhCB05-F were diagnosed with squamous cell carcinoma of the larynx, upper alveolus, and buccal mucosa respectively. While patients MhCL03-F and MhCA04-F presented with primary tumor, patient MhCB05-F was from a recurrent patient. The clinical details of the patients are mentioned in table 1.

Tumor samples (5mm punch) were digested with trypsin for MhCB05-F patient and collagen for MhCL03-F and MhCA04-F patients for 15 min at 37°C after decontamination with povidone-iodine solution (Win Medicare Pvt. Ltd.). The tissue was then chopped into smaller sections and placed in serrated petri dishes in RPMI-1640 medium supplemented with 20% FBS (cat.no. RM10434; HiMedia Laboratories; LLC) and 1X Penicillin-Streptomycin solution and incubated at 37°C with 5% CO_2. Dead cells and debris were removed by changing the culture medium every 48 h. The resulting fibroblast cells were then trypsinized and passaged for more than 40 passages in RPMI complete medium and characterized further. The names have been arrived via an acronym, where, M – Mazumdar shaw medical foundation;

Table 1: Clinical and pathological details of the established cell lines.

Cell line	Patient Age (years)/ sex/habit	Tumor diagnosis	Comorbidity	Tumor Progression
MhCL03-F	65/M/Smoking	Moderately differentiated Squamous cell carcinoma of the Larynx	Diabetes	Presentation: Primary
MhCA04-F	80/M/Drinking and Chewing	Moderately differentiated Squamous cell carcinoma of the upper alveoulus	Diabetes / HTN	Presentation: Primary
MhCB05-F	65/M/Not reported	Moderately differentiated Squamous cell carcinoma of the buccal mucosa	Asthamatic	Presentation: Primary Presentation: Primary tumor in January 2016 treated by surgery and no adjuvant therapy. Recurrence in January 2017

M: male; HTN: hypertension

h – human; C – Cancer of; L – Larynx/A – upper Alveolus/B – Buccal mucosa; 03/04/05 – Patient code; F/E – Fibroblast/Epithelial.

HeLa cell culture

HeLa cells were grown in DMEM medium (#11995-065; Gibco; Thermo Fisher Scientific, Inc.), pH 7.2, supplemented with 10% FBS and 1X penicillin-streptomycin solution at 37 °C with 5% CO_2. The authenticity of HeLa cell line was further confirmed by STR profiling (Table 2).

Growth characteristics

The growth pattern for MhCL03-F, MhCA04-F, and MhCB05-F CAFs was studied by using Alamar blue assay. Cells were seeded at a density of 2×10^3 cells per well in a 96-well plate, and incubated at 37°C for 24h. 12µL of Alamar blue solution (#DAL1025; Invitrogen; Thermo Fisher Scientific, Inc.) was added resulting in a final concentration of 10% followed by an incubation for 18h at 37°C. The fluorescence readings were taken by collecting the supernatant media from the wells in Biotek Synergy H1 Hybrid Multi-Mode reader at 560nm and 590nm as excitation and emission wavelength respectively. The results display the mean ± standard deviation of three independent experiments.

Immunocytochemistry

For detection of HPV by immunocytochemistry, respective cell lines at a concentration of 5×10^3 cells per coverslip were cultured for 24h followed by staining with p16 antibody (#G175-405; Biogeneics; Proteogen) [21]. HeLa cells were used as a positive control for the experiment. Cells were fixed with 4% paraformaldehyde (#GRM3660-500g; HiMEDIA) for 10 min, followed by permeabilization with 0.1% Triton X 100 (cat.no. 10655; Fisher Scientific; Invitrogen) for 10 min at room temperature. Cells were blocked for 1h at room temperature with 1% BSA (#TC194; HiMEDIA laboratories; LLC) in 1X PBS, followed by probing with p16 antibody and incubation at room temperature for 2h. Secondary antibody (#K5007; Dako; Agilent Technologies, Inc.) was added and incubated for 30 min in dark. Visualization was done using 3,3′-Diaminobenzidine, and counterstaining with haematoxylin stain (cat.no. S034; HiMEDIA Laboratories, LLC). Mounting was done using DPX mounting media (#DAL1025; Qualigen Fine Chemicals TM; Thermo Fisher Scientific) and observed under Nikon Eclipse E200 light microscope. The coverslips were washed twice with 1X PBS after every treatment.

HPV PCR

PCR was run to check for the presence of HPV infections in the established CAF cell lines. The primers used were MY09 (5'CGTCCMARRGGAWACTGATC3') and MY11 (5'GCMCAGGGWCATAAYAATGG3') which flanks a 450 bp amplicon. As a control for the reaction, the DNA samples were subjected to PCR to amplify β actin using 5'AGCCATGTACGTTGCTATCCA-3' (Forward primer) and 5' ACCGGAGTCCATCACGATG-3' (Reverse primer) which flanks 120 bp amplicon was the reference gene control. Genomic DNA from HeLa cells was used as a positive control. PCR was set up using template DNA (200 ng), Taq polymerase (#D1806; Sigma-Aldrich; Merck KGaA), 1X PCR buffer, dNTPs (0.2 mM each), and primers (0.1 µM each). The amplification conditions for PCR were: 94°C for 5 min, 95°C for 30 sec (denaturation), 50°C and 60°C for MY09/MY11 and β actin, respectively, for 1 min (annealing) and 72°C for 1 min (elongation). Final elongation step was carried out at 72°C for 10 min. Visualization of amplified PCR products was done via agarose gel electrophoresis (1.5%).

Flow cytometry

1×10^6 cells/100µl were twice washed in PBS, followed by permeabilization with 0.1% triton X 100 (#10655; Thermo Fisher Scientific, Inc.) for half an hour followed by incubation with primary antibodies for 1 h on ice. Anti-FSP1 (#F4771; Sigma-Aldrich; Merck KGaA), EpCAM

Table 2: STR analysis of HeLa cell line. The STR profile matched 100% to HeLa cell line from American Type Culture Collection (ATCC) database https://www.atcc.org/search-str-database as authenticated by TheraCUES.

	Marker	Allele#1	Allele#2
HeLa	TH01	7	7
	D21S11	27	28
	D5S818	11	12
	D13S317	-	-
	D7S820	8	12
	D16S539	9	10
	CSF1PO	9	10
	AMEL	X	X
	vWA	16	18
	TPOX	8	12

(#4545; Cell Signaling Technology; Inc.), CD31 (#303101; Biolegend; Inc.), and CD45 (#361901; Biolegend; Inc.) were used as primary antibodies as per the dilutions instructed by the manufacturer. The cells were then treated with Alexa-488 conjugated secondary antibody (#A11029; Invitrogen; Thermo Fisher Scientific; Inc.) for 30 min in dark at room temperature. The cells were washed twice with 1X PBS after every treatment followed by centrifugation at 500 x g for 5 minutes at 4°C. Unstained cells were used to correct the background fluorescence. The BD FACS Canto II system was used to conduct the experiment in duplicates, and the BDFACS Diva software, version 8.0.1, was used to analyze the results.

Immunofluorescence

Purity of the established CAF cell lines were determined by staining 2×10^4 cells, seeded on a coverslip and incubated overnight, fixed with 4% paraformaldehyde (#GRM3660-500g; HiMEDIA) for 10 min at room temperature, followed by permeabilization with 0.2% triton-X 100 in 1X PBS, blocked with 1% BSA (#TC194; HiMEDIA laboratories; LLC) in 1X PBS for 1h at room temperature, followed by staining with anti-FSP-1,EpCAM, CD31, and CD45 antibodies and incubated for 2h at room temperature. Cells were incubated with Alexa-488 conjugated secondary antibody for 1h in dark at room temperature. DAPI histology mount (#F6057; HiMEDIA laboratories; LLC) was used to mount the coverslips on the slides. The slides were visualized under Zeiss Scope A1 fluorescent microscope using FITC filter. The coverslips were washed with 1X PBS after every treatment.

STR Profiling

In order to determine the genomic identity and to exclude any cross-contamination of cell lines, STR profiling was performed using 10 loci as standard markers. Briefly, the genomic DNA was isolated from 1×10^6 cells from all the cell lines. 50 ng of genomic DNA was used for the profiling. STR multiplex assay was performed by TheraCUES, Bangalore using GenePrint 10 (Promega corporation), version 3.0.0 of the SoftGenetics. GeneMarker_HID was used in order to analyze the result and the data was examined by referring to the STR Database of ATCC and CLASTR.

DNA ploidy determination

Ploidy analysis was used to determine the cell lines' DNA content [21]. Normal cells from a healthy donor were chosen as a diploid control for the experiment because they rarely show any altered DNA content [22] and because their average DNA value has been classified as diploid [23]. The ploidy of the cells was anticipated by determining the DNA index of the cells. The DNA was stained by treating the cells in PBS containing RNase (10 µg/ml; cat. no.12091021; Invitrogen; Thermo Fisher Scientific, Inc.) and Propidium Iodide (40 µg/ml; cat.no. P4170; Sigma- Aldrich; Merck KGaA) at 37°C for 30 min. DNA content was determined in comparison to PBMCs which were used as control (diploid gDNA content). The fluorescence was determined by using BD FACS Canto II system to analyze the cells. The DNA index of the cell lines was estimated by dividing the mean channel of G0 phase cells by the mean channel of the lymphocytes.

Isolation of human lymphocytes

Lymphocytes were isolated from a 32 year healthy female from Rajasthan, India, in December 2022 by collecting whole blood (diluted 1:3 in PBS) and layering above Ficoll Histopaque (#LSM-1077; HiMEDIA Laboratories; LLC) at 1:1 volume/volume ratio followed by centrifugation at 400 x g for 25 min at 20°C. The acceleration and deceleration were maintained at 5 and 6 respectively throughout the procedure. The resultant buffy coat having lymphocytes were further washed with 1X PBS for further processing.

Estimation of proliferation

Epithelial cells (MhCT08-E and MhCT12-E), 1×10^4 cells per well in a 96-well plate were treated with 50% serum free CAF condition medium supplemented with 10% FBS (#10270-106; Gibco) and 50% fresh RPMI medium for 72h. Cell viability was measured with Alamar Blue as described for growth pattern measurement above. Fold proliferation was estimated in comparison to without treatment with CAF conditioned medium. The results display the mean ± standard deviation of three separate experiments.

Invasion assay

For invasion assay, ECM gel (#E1270; Sigma-Aldrich; Merck KGaA) was prepared in RPMI serum-free media at a final concentration of 1mg/mL. Cell culture inserts with a pore size of 8.0 µm (#TCP083; HiMEDIA Laboratories, LLC) were coated with 100 µl of ECM and incubating at 37 °C for 3-4h, followed by seeding the cells on the apical chamber (over the ECM gel) with a density of 1×10^4 epithelial cells per insert. Neat CAF Condition media was added in the basolateral chamber. The cells were allowed to invade for a period of 48 h and prepared for imaging by separating the cells on the inside of the insert using a cotton swab. Fixing of the cells was done by using 4% paraformaldehyde at room temperature for 10 min. The cells were then stained with 2% crystal violet for 5 min at room temperature. Any unbound dye was removed by washing it thrice with 1X PBS. The cells were then air-dried and imaged. The inserts were incubated in 10% acetic acid (#Q21057; Qualigen; Thermo Fisher Scientific, Inc.) in water while shaking at room temperature for 10 min to extract bound crystal violet for invasion quantitation. Absorbance was read at 590nm by transferring the extract into a 96-well microplate. The results display the mean ± standard deviation of three independent experiments.

Sphere formation assay

A total of 5×10^3 cells were seeded in the ultra-low (#3473; Corning; Inc.) attachment plate along with the CAF conditioned medium. The cells were observed at 5th day for their sphere formation ability and images were captured using bright field Nikon microscope. Size of the spheres was calculated using the formula $4/3\pi r^3$, where 'r' is the geometric mean of the two longest diameters of the spheres as calculated using Fiji ImageJ software vs. 1.53t.

Collection of Conditioned medium

CAFs were cultured in 6 well plates (#140675; Thermo Fisher Scientific; Inc.) in complete RPMI until 80% confluency followed by changing the culture medium to serum free. Conditioned medium (CM) was collected after 48h. of culturing the cells in complete RPMI medium without FBS, supplemented with 1X PenStrep and 1X GlutaMax.

Statistical analysis

The mean and standard error of the mean are used to express all quantitative data. Unless otherwise noted, statistical significance was determined using the paired Student's t-test. $P < 0.05$ was taken into consideration to show a statistically significant difference. All the statistical calculations were performed using GraphPad Prism software (version 5.00; GraphPad Software, Inc.).

Results

Characterization of established cell lines

Growth Characteristics: The three cell lines revealed a similar growth pattern as shown in figure 1A, wherein steady growth was observed until day 5. MhCB05-F exhibited a more profound growth followed by MhCA04-F and MhCL03-F.

Morphology: The morphology of the established CAF cells was determined by staining them with haematoxylin and further observing under light microscope. As shown in figure 1B, the cells exhibited a typical elongated, spindle shaped morphology [28,29], consistent with the fibroblast morphology.

Ploidy Determination: DNA index was calculated as the ratio of the mean fluorescent intensity of the CAFs and healthy diploid lymphocytes in G0/G1 phase. Upon analysis it was observed that MhCL03-F, MhCA04-F and MhCB05-F cells had DNA indices of 1.2, 1.3, and 0.94 respectively (Figure 1C). The findings suggested that the patient samples contain aberrant DNA, which may be why the cells immortalized spontaneously.

Purity: In order to use a cell line as a study model, it is important to authenticate and confirm the purity of the cell lines established. The cell lineage of the potential cancer-associated fibroblast was determined by confirming the expression of fibroblast-specific markers via flow cytometric analysis. As shown in figure 2A, the CAF nature of the cell lines was confirmed by positive staining with Fibroblast specific protein – 1 (FSP-1) antibody. Similarly, the origin of CAFs was also confirmed by negative staining with EpCAM antibody which is specific against epithelial cells [30]. FACS analysis results revealed that, MhCL03-F, MhCA04-F, and MhCB05-F exhibited a percentage positivity of 99.7%, 95.2%, and 89.4% for FSP-1 respectively. Whereas, < 0.1% positivity was observed for EpCAM expression. The purity of cell lines was also determined via immunofluorescent analysis (Figure 2B). The cells showed positive staining for FSP-1 antibody which is specific against fibroblast cells. Negative staining of the cells against EpCAM, CD31, and CD45 antibodies which are specific to epithelial cells, endothelial cells and leucocytes respectively, confirmed the CAF nature of the established cell lines [31]. Less than 0.1% population positivity in flow cytometry analysis of the cells with CD31 and CD45 antibodies confirmed further the fibroblast lineage (Figure 2C). Human lymphocytes were used as positive control and MhCT12-E and MhCT08-E epithelial cells [26] were used as a negative control for FSP-1 staining and positive control for EpCAM staining. Overall, the results conclude and confirm the purity of established CAF cell lines.

STR profiling: In order to indicate the distinctiveness of the cell lines from those that are present in ATCC and CLASTR database, STR profiling was done. As depicted in table 3, none of the cell lines matched with the established cell line databases, and each other, indicating their novelty and excluding any cross contamination.

Detection of HPV: HPV infections are recognized as one of the major factors leading to HNSCC. It has been studied that, HPV positive HNSCCs exhibits a much convenient prognosis when compared to HPV negative cancers [32]. Thus, it becomes important to determine the HPV infection status of an established cell line. Immunocytochemistry analysis was carried out to determine the status of HPV infection, wherein expression of p16 antigen was examined [27]. Upon PCR and immune-cyto-chemical analysis, it was observed that, all the three cell lines were stained negative for p16 antibody (Supplementary Figure 1A) as no nuclear stain with the p16 antigen was observed in any of the established cultures, while the HeLa culture stained positively with the same. HPV negative status of the established cell lines was further confirmed by PCR as no amplified bands were observed (Supplementary Figure 1B), however, a 120bp amplicon was observed in beta actin control.

Tumorigenic properties of established cell lines

Several assays, by treating the epithelial cells with CAF condition medium, were carried out to determine the tumorigenic potential,

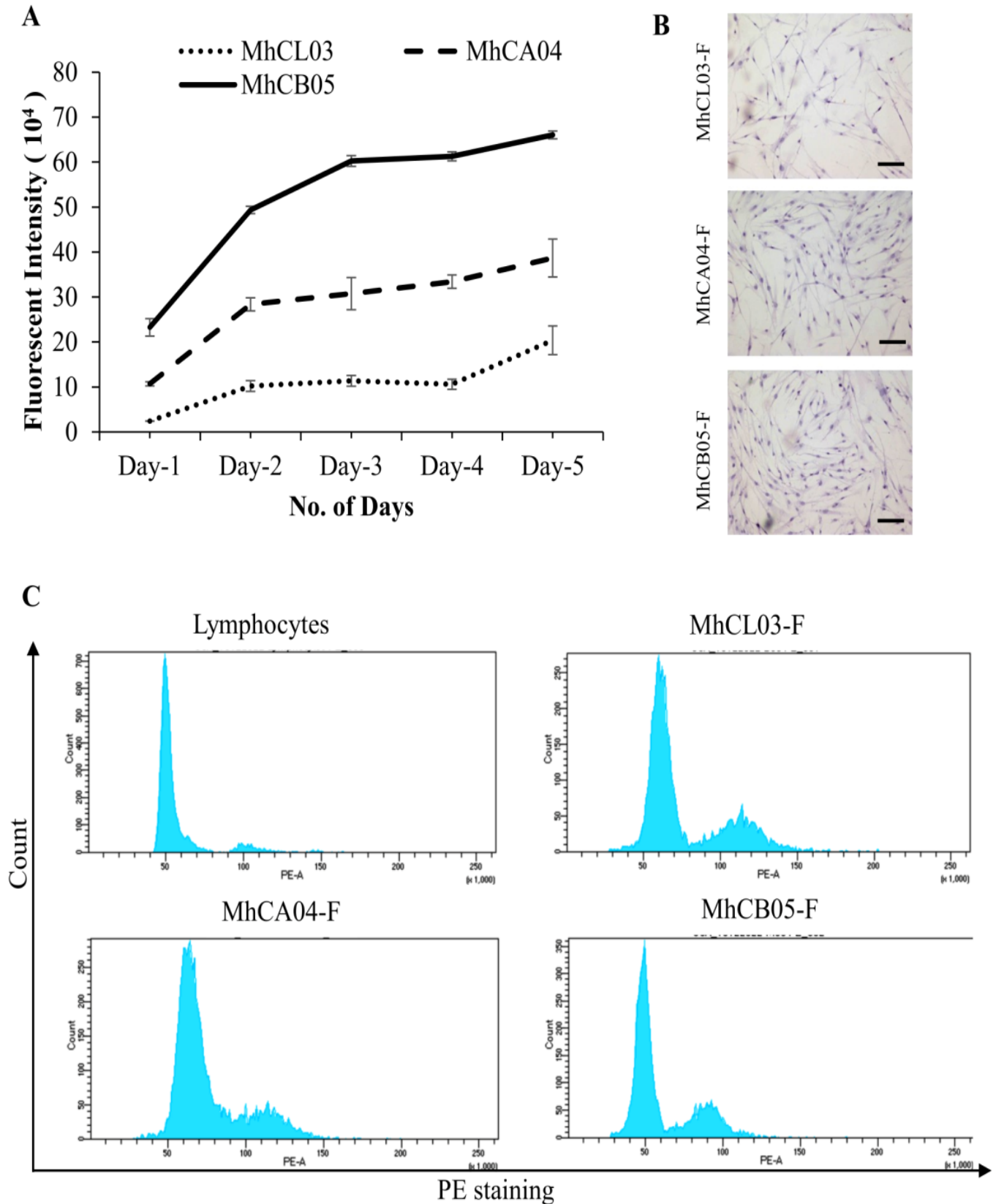**Estimation of proliferation:** Upon treatment with CAF

Figure 1: Characterization of established cell lines. (A) Growth pattern of MhCL03-F, MhCA04-F, and MhCB05-F cell lines. (B) Microscopic images of Hematoxylin stained cells exhibiting spindle shaped morphology (Magnification 4X, Scale bar- 100μm). (C) Determination of ploidy by flow cytometry analysis. Human lymphocytes, MhCL03-F, MhCA04-F, and MhCB05-F stained with propidium iodide.
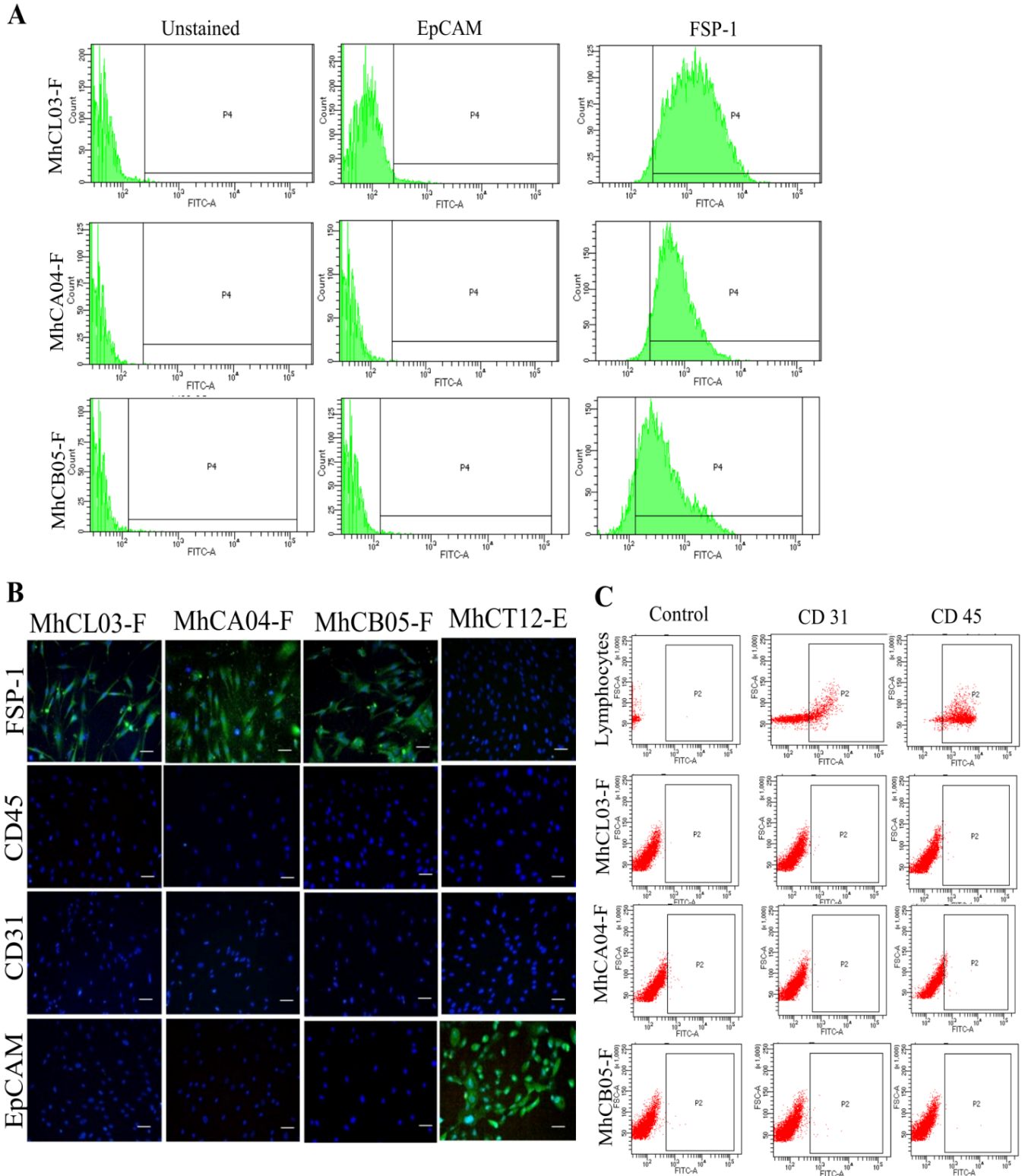
Figure 2: Purity of established cell lines. (A) FACS analysis displaying EpCAM and FSP-1 staining for the established cell lines. (B) Fluorescent images of established cell lines stained with FSP-1, EpCAM, CD31, and CD45 (Magnification 10X, Scale bar- 50μm). (C) FACS analysis displaying CD31 and CD45 staining for the lymphocytes and the established lines as indicated.

Table 3: Proof of novelty of established cell lines by STR (<55% match cut-off from ATCC, CLASTR public databases, and among themselves)

Sample Name	Marker	Parental Allele#1	Passage / Daughter Allele#1	Parental Allele#2	Passage / Daughter Allele#2	% Match
MhCL03-F & MhCA04-F	TH01	9	7	9	7	40
	D21S11	31	30	31.2	31.2	
	D5S818	11	11	13	11	
	D13S317	8	8	8	10	
	D7S820	8	10	11	12	
	D16S539	9	9	10	11	
	CSF1PO	11	11	12	13	
	AMEL	X	X	Y	Y	
	vWA	17	15	18	17	
	TPOX	8	8	10	9	
MhCA04-F & MhCB05-F	TH01	7	9	7	-	42.11
	D21S11	30	28	31.2	32.2	
	D5S818	11	11	11	11	
	D13S317	8	8	10	12	
	D7S820	10	8	12	11	
	D16S539	9	13	11	13	
	CSF1PO	11	10	13	12	
	AMEL	X	X	Y	Y	
	vWA	15	15	17	18	
	TPOX	8	8	9	9	
MhCL03-F & MhCB05-F	TH01	9	9	9	-	52.6
	D21S11	31	28	31.2	32.2	
	D5S818	11	11	13	11	
	D13S317	8	8	8	12	
	D7S820	8	8	11	11	
	D16S539	9	13	10	13	
	CSF1PO	11	10	12	12	
	AMEL	X	X	Y	Y	
	vWA	17	15	18	18	
	TPOX	8	8	10	9	

ACTC: American Type Culture Collection; CLASTR: Cellosarus STR similarity search tool; E: epithelial; F: fibroblast

conditioned medium, a significant increase in proliferation of epithelial cells was observed (P<0.01) as compared to the no treatment control, wherein maximum significant proliferation was seen at 48h for all the five cell lines (Figure 3A). Upon comparison between five CAFs (Figure 3A), it was observed that the MhCA04-F (upper alveolus) conditioned medium had the best and most significant effect on the induction of proliferation in both the MhCT12-E and MhCT08-E cell lines. MhCL03-F (Larynx) and MhCB05-F (Buccal Mucosa) conditioned medium followed next, while MhCT08-F (Tongue) and MhCT12-F (Tongue) conditioned medium were

similar to MhCB05. The demonstration of site-independent action of the CAFs are novel and intriguing. Interestingly, MhCT08-E cell line showed higher proliferation after 24 h of treatment with CAF conditioned medium as compared to MhCT12-E cell line. However, proliferation rate of MhCT12-E cell line increased dramatically as compared to MhCT08-E cell line upon prolonged treatment with indicated conditioned medium. This may be due to a receptor mediated signal transduction event caused by a "CAF factor" in MhCT12-E, which is absent in MhCT08-E.
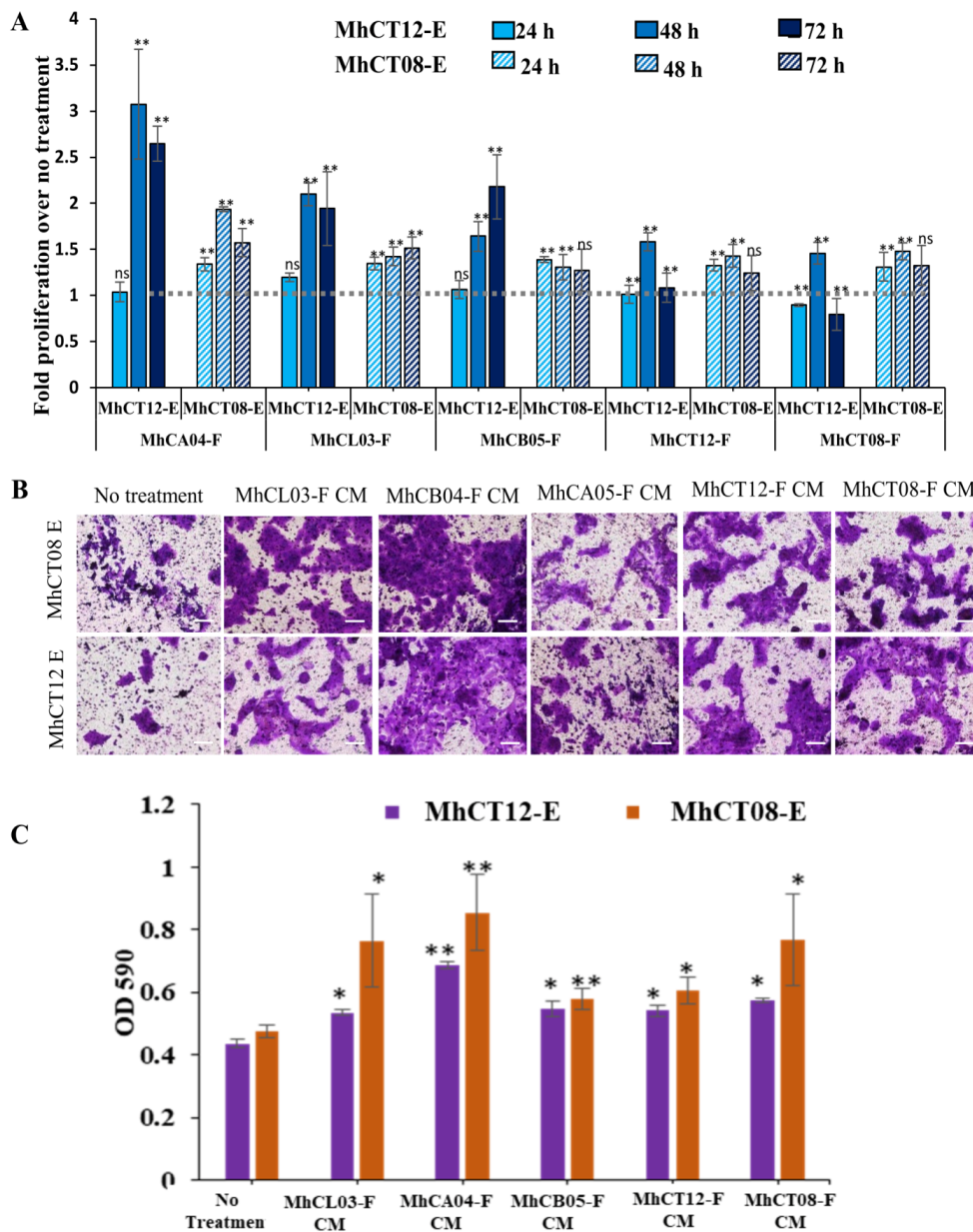

Figure 3: Tumorigenic properties of established CAF cell lines. (A) C Proliferative potential of MhCT12-E and MhCT08-E under the influence of indicated conditioned medium. The grey line intersection depicts the no treatment control for both the epithelial cells. Statistical significance over no treatment, where, *p<0.05 and **p<0.01 (B) Invasive potential of epithelial cells under the influence of CAF condition medium (Magnification 10X, Scale bar- 100μm). (C) Graphical illustration of the invasive effect of CAFS on epithelial cells. CM- Conditioned medium, E-Epithelial, F- Fibroblast

Citation: Nehanjali Dwivedi, Hafsa Bahaar, DN Shashank, Christine Elizabeth Cherry, Charitha Gangadharan, Amritha Suresh, Moni A Kuriakose, Vijay Pillai, Smitha PK, and Manjula Das. Novel cancer associated fibroblasts from diverse locales enhance the tumorigenicity of tongue Tumor Epithelia. Dental Research and Oral Health. 6 (2023): 65-78.
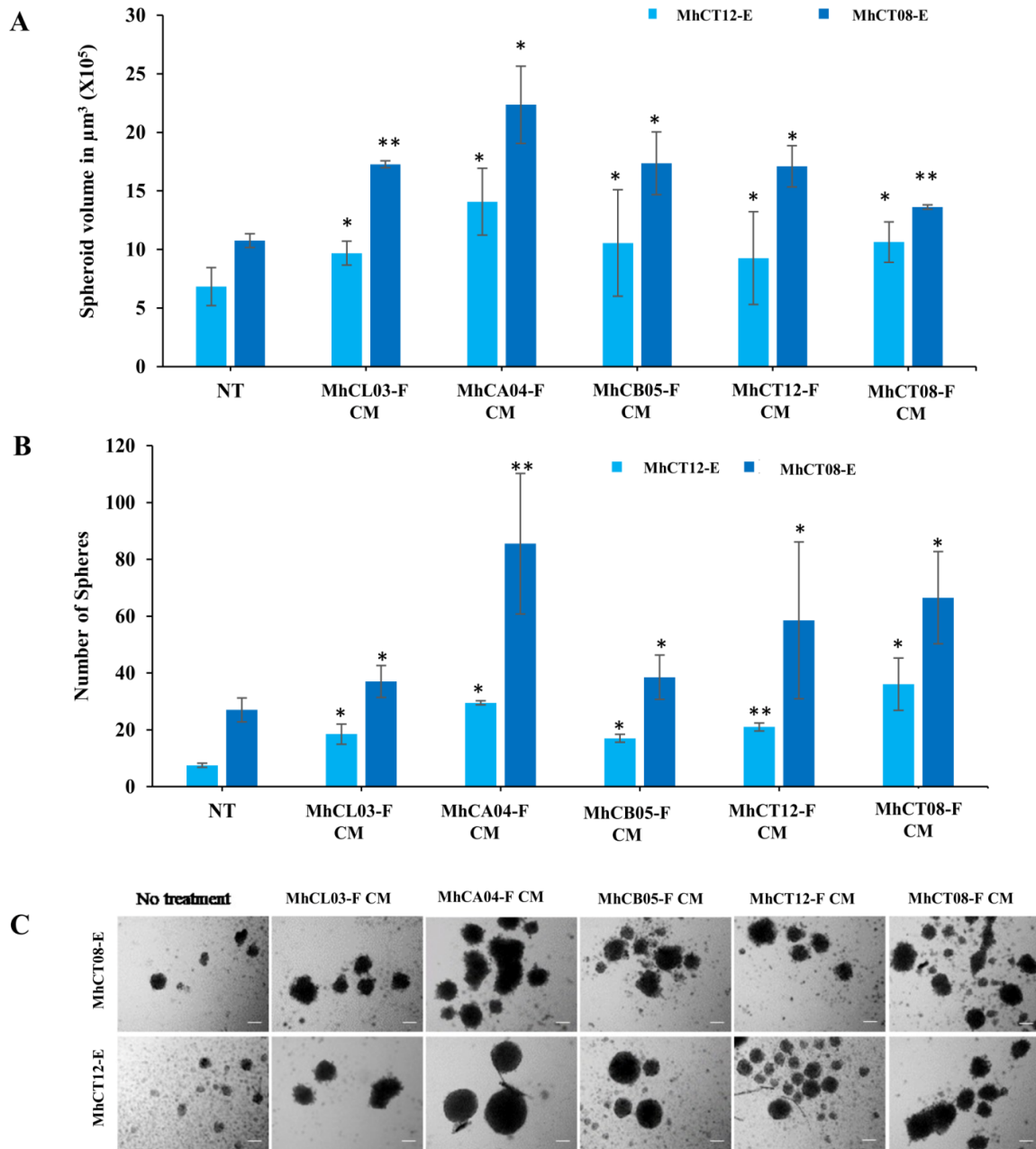
Figure 4: Sphere formation assay. (A) Volume of MhCT08-E and MhCT12-E spheres formed under the effect of CAF conditioned mediums as indicated (*p<0.1,**p<0.05) , (B) Sphere forming potential of MhCT08-E and MhCT12-E cells under the influence of CAF condition medium as indicated (*p<0.05 and **p<0.01), Statistical significance indicates difference between no treatment and CAF conditioned medium treatment (C) Sphere formation potential of MhCT08-E and MhCT12-E cells under the influence of CAF condition medium. (Magnification 10X, Scale bar-100μm), CM-Condition media, NT-NoTreatment, F–Fibroblast, E–Epithelial

Invasion assay: A significant increase in the invasive potential of MhCT12-E and MhCT08-E epithelial cells was observed upon treatment with CAF condition medium (Figure 3B and 3C). Upon quantification, it was observed that the maximum invasion by both the epithelial cells was observed under the influence of MhCA04-F condition medium followed by MhCL03-F, MhCB05-F, MhCT08-F and MhCT12-F conditioned medium in decreasing order as compared to the no treatment control.

Sphere formation: Sphere formation potential of epithelial cells increased under the influence of CAF condition medium (Figure 4). Upon analysis it was observed that not only the size (Figure 4A), but also the total number (Figure 4B) of the spheres increased upon treatment with CAF conditioned medium as compared to the no treatment group. Similar to the other tumorigenicity assays, the effect of the MhCA04-F CAF conditioned medium was the most profound followed by MhCL03-F, MhCA05-F, MhCT08-F and MhCT12-F

Citation: Nehanjali Dwivedi, Hafsa Bahaar, DN Shashank, Christine Elizabeth Cherry, Charitha Gangadharan, Amritha Suresh, Moni A Kuriakose, Vijay Pillai, Smitha PK, and Manjula Das. Novel cancer associated fibroblasts from diverse locales enhance the tumorigenicity of tongue Tumor Epithelia. Dental Research and Oral Health. 6 (2023): 65-78.

conditioned medium, with the total number of spheres of 93, 40, 42, 57 and 66 in case of MhCT08-E cells (Figure 4B). Similarly, treatment with MhCL03-F, MhCA04-F, MhCB05-F, MhCT12-F and MhCT08-F condition medium resulted in a total of 19, 29, 17, 21 and 36 spheres respectively in MhCT12-E cells and (Figure 4B). Additionally, as per the previous report, it was also observed that MhCT08-E formed much larger and number of spheres under the influence of CAF condition medium when compared to MhCT12-E cells (Figure 4C).

Discussion

Over the past decade it has become evident that TME encourages tumor growth [33]. Concern has been raised about the ECM's constituent parts and mechanical attributes as significant catalysts for the behavior of cancer cells and the development of the disease. CAFs are a crucial component of TMEs and are essential for matrix remodeling [34]. CAFs are responsible for the secretion of multiple growth factors, kinases, cytokines, and chemokines into the TME to facilitate tumor progression [22,35-37]. Thus establishment of CAF cell lines from HNSCC will be of immense value to the scientific community and eventually to the clinic through translational research. Development of cell lines from head and neck cancer patients from India has greatly advanced the understanding of tumor heterogeneity and revealed the molecular variations between the Indian (Asian) and Western populations, caused may be due to genetic variations [38]. A source of cancer cells with the heterogeneity of the cell populations present in the parental tumor may be found in the cell lines developed from patients. Notably, they can be utilized to comprehend the molecular processes underlying cancer cells' resistance to chemotherapy and radiation treatment [39]. In the current investigation, three Indian males with known risk factors diagnosed with squamous cell carcinoma of the larynx, buccal mucosa, and upper alveolus were used to produce and characterize three unique CAF cultures. Primary cultures have been developed using a variety of techniques. Some studies mention seeding the cell suspension and directly digesting the tumor tissue [18,40], Using a mouse xenograft model, Mulherkar et al. [41] created NT8e, an oral squamous cell cancer cell line. Explant culture was used in the current investigation, as has been described before [39,42-45]]. Several studies have described the isolation of CAF primary cultures from several areas of the oral cavity, including the gingivo-buccal mucosa, tongue, retromolar area, palate, and other places such as the lip, jaw, soft palate, and so on [21-25]. However, ours is the second study reporting establishment of CAF cell line from various regions of head and neck cancer apart from the tongue carcinoma CAFs reported earlier by the authors [26].

According to a recent study, different media can be used to promote the populations of fibroblasts and epithelial cells to develop at different rates [46]. However, to avoid any phenotypic or genotypic changes brought on by patient-derived xenograft generations, the cultures described in the present investigation were grown in RPMI-1640 complete media. These cultures did not require any feeder cells or viral vectors to be stabilized spontaneously. The cell lines stained positive for FSP-1 via both the immunocytochemical and flow cytometric analysis. Additionally, while endothelial and fibroblast cells have a very similar appearance, negative staining with the endothelium specific (CD31) and hematopoietic specific (CD45) markers disproved their suspicion of cross contamination in the established cultures and proving their fibroblast specific lineage. These CAFs could be decisively defined as cells negative for epithelial (EpCAM), endothelial (CD31) and leukocyte (CD45) markers with an elongated morphology [31]. An insight of the aggressiveness, potential for metastasis, and prognosis of the disease can be gained through DNA ploidy analysis of cancer cells [47-49]. The three cell lines contained aneuploid DNA compared to the lymphocytes' diploid DNA. Uncontrolled cell divisions lead to aberrant karyokinesis, raising the ploidy level of the cells [50]. In this study we observed that even though the CAFs were from different head and neck sites, upon co-culture, they were still able to increase the tumorigenicity of both the epithelial cells derived from tongue squamous cell carcinoma, a different site altogether. This implies that these CAFs are not restricted in imparting the increased tumorigenicity to a particular site, but may also be used to study tumor progression from a number of sites in oral cancer, or may even be expanded to pan cancer studies, making them an immensely useful tool. This may be due to various signaling factors released by the CAFs, which promote tumorigenesis and establishes these cells as an effective model to study tumor-stroma crosstalk. Additionally, the CAFs themselves can serve as excellent model systems for studying tumor evolution. However, the study is limited to in-vitro potential so far.

Conclusion

In conclusion, the cell lines generated in this work show consistent cell shape and enduring growth capacity. Along with the two autologous pairs established by the group earlier, they offer a practical tool for doing basic and translational research in the area of tumor-stroma interaction in head and neck cancer, in addition to having the potential to be employed as a novel drug testing platform in co-culture settings. The study, for the first time, reports the site-independent ability of CAFs to promote tumorigenicity.

Acknowledgements

Funding

Availability of data and materials

All the data generated as a part of the study has been submitted along with the manuscript.

Authors' contributions

Authors MD and AS conceived the idea of the study. Authors MAK and VP provided the samples. Author CG collected the samples and isolated the cell types. Author ND maintained, cultured and characterized the cell types. Authors ND, HB and DNS performed the tumorigenecity experiments with help from author CEC under the guidance of SPK. Authors ND and HB wrote the manuscript and analyzed the data. Figures were prepared by authors ND, HB and DNS. Authors SPK and MD reviewed the manuscript. All the authors read and approved the manuscript.

Ethics approval and consent to participate

The present study was approved [approval no. NHH/MEC-CL-2015-405 (A)] by the ethics committee of Narayana Health (Bangalore, India).

Patient consent for publication

Informed consent for the study was obtained from all the patients involved in the study.

Competing interests

The authors declare that they have no competing interests.

References

1. Sung H, Ferlay J, Siegel RL, et al. Global Cancer Statistics 2020: GLOBOCAN Estimates of Incidence and Mortality Worldwide for 36 Cancers in 185 Countries. CA Cancer J Clin 71 (2021): 209-249.

2. Lala M, Chirovsky D, Cheng JD et al. Clinical outcomes with therapies for previously treated recurrent/metastatic head-and-neck squamous cell carcinoma (R/M HNSCC): A systematic literature review. Oral Oncol 84 (2018): 108-120.

3. Jethwa AR and Khariwala SS. Tobacco-related carcinogenesis in head and neck cancer. Cancer Metastasis Rev 36 (2017): 411-423.

4. Kulkarni MR. Head and Neck Cancer Burden in India. Int J Head Neck Surg 4 (2013): 29-35.

5. Kobayashi K, Hisamatsu K, Suzui N, et al. A Review of HPV-Related Head and Neck Cancer. J Clin Med 7 (2018): 128.

6. Ramqvist T, Grün N, Dalianis T. Human papillomavirus and tonsillar and base of tongue cancer. Viruses 7 (2015): 1332-1343.

7. Chaturvedi AK, Engels EA, Pfeiffer RM, et al. Human papillomavirus and rising oropharyngeal cancer incidence in the United States. J Clin Oncol 29 (2011): 4294-4301.

8. Iype EM, Pandey M, Mathew A, et al. Oral cancer among patients under the age of 35 years. J Postgrad Med 47 (2001): 171-176.

9. Kulkarni MR. Head and Neck Cancer Burden in India. Int J Head Neck Surg 4 (2007): 29-35.

10. Johnson DE, Burtness B, Leemans CR, et al. Head and neck squamous cell carcinoma. Nat Rev Dis Prim 6 (2020): 1-22.

11. Tlsty TD, Coussens LM. Tumor stroma and regulation of cancer development. Annu Rev Pathol 1 (2006): 119-150.

12. Liu M, Casimiro MC, Wang C, et al. p21 CIP1 attenuates Ras- and c-Myc-dependent breast tumor epithelial mesenchymal transition and cancer stem cell-like gene expression in vivo. Proc Natl Acad Sci 106 (2009): 19035-19039.

13. Cirri P and Chiarugi P. Cancer associated fibroblasts: the dark side of the coin. Am J Cancer Res 1 (2011): 482-497.

14. Miserocchi G, Mercatali L, Liverani C, et al. Management and potentialities of primary cancer cultures in preclinical and translational studies. J Transl Med 15 (2017): 229.

15. Bremnes RM, Dønnem T, Al-Saad S, et al. The Role of Tumor Stroma in Cancer Progression and Prognosis: Emphasis on Carcinoma-Associated Fibroblasts and Non-small Cell Lung Cancer. J Thorac Oncol 6 (2011): 209-217.

16. Ni Y, Zhou X, Yang J, et al. The Role of Tumor-Stroma Interactions in Drug Resistance Within Tumor Microenvironment. Front Cell Dev Biol 20 (2021): 1206.

17. Bussard KM, Mutkus L, Stumpf K, et al. Tumor-associated stromal cells as key contributors to the tumor microenvironment. Breast Cancer Res 18 (2016): 1-11.

18. Tatake RJ, Rajaram N, Damle RN, et al. Establishment and characterization of four new squamous cell carcinoma cell lines derived from oral tumors. J Cancer Res Clin Oncol 116 (1990): 179-186.

19. Zhao M, Sano D, Pickering CR, et al. Assembly and Initial Characterization of a Panel of 85 Genomically Validated Cell Lines from Diverse Head and Neck Tumor Sites. Clin Cancer Res 17 (2011): 7248-7264.

20. Hayes TF, Benaich N, Goldie SJ, et al. Integrative genomic and functional analysis of human oral squamous cell carcinoma cell lines reveals synergistic effects of FAT1 and CASP8 inactivation. Cancer Lett 383 (2016): 106-114.

21. Patel AK, Vipparthi K, Thatikonda V, et al. A subtype of cancer-associated fibroblasts with lower expression of

alpha-smooth muscle actin suppresses stemness through BMP4 in oral carcinoma. Oncog 7 (2018): 1-15.

22. Datar UV, Kale AD, Angadi P V, et al. Role of cancer-associated fibroblasts in oral squamous cell carcinomas, surgical margins, and verrucous carcinomas: An immunohistochemical study. J Clin Transl Res 8 (2022): 80-85.

23. Li H, Zhang J, Chen SW, et al. Cancer-associated fibroblasts provide a suitable microenvironment for tumor development and progression in oral tongue squamous cancer. J Transl Med 13 (2015): 1-10.

24. Yang J, Shi X, Yang M, et al. Glycolysis reprogramming in cancer-associated fibroblasts promotes the growth of oral cancer through the lncRNA H19/miR-675-5p/PFKFB3 signaling pathway. Int J Oral Sci 13 (2021): 1-11.

25. Zhang JY, Zhu WW, Wang MY, et al. Cancer-associated fibroblasts promote oral squamous cell carcinoma progression through LOX-mediated matrix stiffness. J Transl Med 19 (2021): 1-16.

26. Dwivedi N, Gangadharan C, Pillai V, et al. Establishment and characterization of novel autologous pair cell lines from two Indian non-habitual tongue carcinoma patients. Oncol Rep 48 (2022): 1-12.

27. Wang H, Zhang Y, Bai W, et al. Feasibility of Immunohistochemical p16 Staining in the Diagnosis of Human Papillomavirus Infection in Patients With Squamous Cell Carcinoma of the Head and Neck: A Systematic Review and Meta-Analysis. Front Oncol 10 (2020): 1-13.

28. Sahai E, Astsaturov I, Cukierman E, et al. A framework for advancing our understanding of cancer-associated fibroblasts. Nat Rev Cancer 20 (2020): 174-186.

29. Liu T, Han C, Wang S, et al. Cancer-associated fibroblasts: An emerging target of anti-cancer immunotherapy. J Hematol Oncol 12 (2019): 1-15.

30. Nurmik M, Ullmann P, Rodriguez F, et al. In search of definitions: Cancer-associated fibroblasts and their markers. Int J Cancer 146 (2020): 895-905.

31. Han C, Liu T, Yin R. Biomarkers for cancer-associated fibroblasts. Biomark Res 8 (2020): 1-8.

32. Nagel R, Martens-De Kemp SR, Buijze M, et al. Treatment response of HPV-positive and HPV-negative head and neck squamous cell carcinoma cell lines. Oral Oncol 49 (2013): 560-566.

33. Kalluri R. The biology and function of fibroblasts in cancer. Nat Rev Cancer 16 (2016): 582-598.

34. Zeltz C, Primac I, Erusappan P, et al. Cancer-associated fibroblasts in desmoplastic tumors: emerging role of integrins. Semin Cancer Biol 62 (2020): 166-181.

35. Zhang JY, Zhu WW, Wang MY, et al. Cancer-associated fibroblasts promote oral squamous cell carcinoma progression through LOX-mediated matrix stiffness. J Transl Med 19 (2021): 513.

36. Li H, Zhang J, Chen SW, et al. Cancer-associated fibroblasts provide a suitable microenvironment for tumor development and progression in oral tongue squamous cancer. J Transl Med 13 (2015): 198.

37. Li Y, Tao Y, Gao S, et al. Cancer-associated fibroblasts contribute to oral cancer cells proliferation and metastasis via exosome-mediated paracrine miR-34a-5p. EBioMedicine 36 (2018): 209-220.

38. Vigneswaran N, Williams MD. Epidemiologic Trends in Head and Neck Cancer and Aids in Diagnosis. Oral Maxillofac Surg Clin North Am 26 (2014): 123-141.

39. Gawas NP, Navarange SS, Chovatiya GL, et al. Establishment and characterization of novel human oral squamous cell carcinoma cell lines from advanced-stage tumors of buccal mucosa. Oncol Rep 41 (2019): 2289-2298.

40. Hamid S, Lim KP, Zain RB, et al. Establishment and characterization of Asian oral cancer cell lines as in vitro models to study a disease prevalent in Asia. Int J Mol Med 19 (2007): 453-460.

41. Mulherkar R, Goud AP, Wagle AS, et al. Establishment of a human squamous cell carcinoma cell line of the upper aero-digestive tract. Cancer Lett 118 (1997): 115-121.

42. Pansare K, Gardi N, Kamat S, et al. Establishment and genomic characterization of gingivobuccal carcinoma cell lines with smokeless tobacco associated genetic alterations and oncogenic PIK3CA mutation. Sci Rep 9 (2019): 1-10.

43. Kaur J and Ralhan R. Establishment and characterization of a cell line from smokeless tobacco associated oral squamous cell carcinoma. Oral Oncol 39 (2003): 806-820.

44. Patil TT, Kowtal PK, Nikam A, et al. Establishment of a Tongue Squamous Cell Carcinoma Cell Line from Indian Gutka Chewer. J Oral Oncol 12 (2014): 1-9.

45. García-Inclán C, López-Hernández A, Alonso-Guervós M, et al. Establishment and genetic characterization of six unique tumor cell lines as preclinical models for sinonasal squamous cell carcinoma. Sci Rep 4 (2014): 4925.

46. Oppel F, Shao S, Schürmann M, et al. An Effective Primary Head and Neck Squamous Cell Carcinoma In Vitro Model. Cells 8 (2019): 555.

47. Stell PM. Ploidy in head and neck cancer: A review and meta-analysis. Clin Otolaryngol 16 (1991): 510-516.

48. Cooke L, Cooke T, Bootz F, et al. Ploidy as a prognostic indicator in end stage squamous cell carcinoma of the head and neck region treated with cisplatinum. Br J Cancer 61 (1990): 759-762.

49. Slootweg PJ, Rutgers DH, Wils IS. DNA ploidy analysis of squamous cell head and neck cancer to identify distant metastasis from second primary. Head Neck 14 (1992): 464-466.

50. Vitale I, Galluzzi L, Senovilla L, et al. Illicit survival of cancer cells during polyploidization and depolyploidization. Cell Death Differ 18 (2011): 1403-1413.